

An in vitro model of hepatitis C virus genotype 3a-associated triglycerides accumulation

Karim Abid^{1,†,‡}, Valerio Paziienza^{1,2,†}, Andrea de Gottardi¹, Laura Rubbia-Brandt³,
Beatrice Conne⁴, Paolo Pugnale¹, Christine Rossi¹, Alessandra Mangia², Francesco Negro^{1,3,*}

¹Division of Gastroenterology and Hepatology, University Hospital, 24 rue Micheli-du-Crest, CH-1211 Geneva, Switzerland

²Division of Gastroenterology, Ospedale 'Casa Sollievo della Sofferenza', S. Giovanni Rotondo, Italy

³Division of Clinical Pathology, University Hospital, Geneva, Switzerland

⁴Department of Medical Genetics and Development, University of Geneva School of Medicine, Geneva, Switzerland

Background/Aims: The hepatitis C virus (HCV) induces lipid accumulation in vitro and in vivo. Although clinical observations are consistent with a direct effect of HCV genotype 3a on lipid metabolism, experimental systems have focused on the expression of HCV proteins of genotype 1. To extend these observations, we established an in vitro model expressing the HCV core of different genotypes.

Methods: The HCV core protein from patients with severe (genotype 3a) or no (genotypes 1b, 2a, 3h, 4h and 5a) liver steatosis was expressed in Huh7 cells. Core protein expression (by immunohistochemistry and immunoblot) and triglycerides accumulation (by Oil Red O stain and enzymatic measurement) were evaluated 48 h after transfection.

Results: Although triglyceride accumulation occurred with genotypes 1b, 3a and 3h, the genotype 3a core protein expression resulted in the highest level of accumulation (i.e. about 3-fold with respect to 1b, and 2-fold with respect to 3h). This effect was not related to core protein expression levels and was abolished by culturing cells in lipid-free medium.

Conclusions: Consistent with observations in chronic hepatitis C patients, the in vitro expression of HCV genotype 3a core protein is the ideal candidate model for studying the mechanisms of HCV-associated steatosis.

© 2005 European Association for the Study of the Liver. Published by Elsevier B.V. All rights reserved.

Keywords: Hepatitis C virus; Genotypes; Steatosis; Chronic hepatitis; Liver fibrosis

1. Introduction

The hepatitis C virus (HCV) is a member of the *Flaviviridae* family and a major cause of chronic liver disease worldwide [1]. Progression of chronic hepatitis C to cirrhosis and hepatocellular carcinoma is influenced by

several cofactors, encompassing male gender, age at infection, excess alcohol drinking [2], obesity [3], coinfection with the hepatitis B virus [4] or the human immunodeficiency virus [5]. Moreover, retrospective studies have shown an association between presence and severity of steatosis and advanced fibrosis [6–9]. Thus, there is a considerable interest in dissecting the mechanism of steatosis in HCV infection, especially in relationship with other metabolic disturbances associated with HCV, such as insulin resistance [11].

Steatosis is frequent in hepatitis C [12]. Its pathogenesis is due to both viral and host factors. Viral steatosis is mostly reported in patients with genotype 3a, in whom fat accumulation correlates with HCV replication level in serum [6] and liver [13], and disappears after successful antiviral therapy [10,12,14,15], strongly suggesting a direct

Received 15 October 2004; received in revised form 7 December 2004; accepted 22 December 2004; available online 11 March 2005

* Corresponding author. Address: Divisions of Gastroenterology and Hepatology and of Clinical Pathology, Hôpital Cantonal Universitaire, 24 rue Micheli-du-Crest, CH-1211 Genève 14, Switzerland. Tel.: +41 22 3729340; fax: +41 22 3729366.

E-mail address: negro-francesco@diogenes.hcuge.ch (F. Negro).

† K.A. and V.P. have contributed equally to this work.

‡ Current address: Department of Neurology, University of Texas Medical Branch, Galveston, TX 77555-0646, USA.

role of specific viral products in the fat deposition. On the other hand, most steatosis of mild intensity observed in patients infected with genotypes other than 3a seems to recognize a metabolic pathogenesis, its most significant clinical correlate being overweight [6]. The latter kind of steatosis tends to decrease the odds of a virological response to antivirals [10]. Its persistence in patients who respond suggests the lack of a role of HCV in its pathogenesis [10,14].

HCV has a single stranded, positive polarity RNA encoding for a polyprotein precursor of about 3000 amino acids, which is further cleaved into 10 mature proteins. Among these, the structural protein implicated in the nucleocapsid assembly, referred to as core protein, was shown to induce steatosis in transgenic mice [16] and to be associated with lipid droplets *in vitro* [17–19]. The fact that the constructs used in these experimental models were derived from isolates of HCV genotype 1b is in apparent conflict with the clinical observation of the significant association of steatosis with HCV genotype 3a. To address this apparent discrepancy, we established an *in vitro* model to study the effect of the core protein belonging to several viral genotypes (1b, 2a, 3a, 3h, 4h and 5a) on lipid accumulation.

2. Materials and methods

2.1. Patients

We selected six patients with chronic hepatitis C, infected with HCV genotypes 1 through 5, including our recently characterized genotype 3h from Somalia [20]. Clinical, virological and histological features are shown in Table 1. All patients underwent liver biopsy during diagnostic workup of their HCV infection. At histology, only patient #3, infected with genotype 3a, had severe steatosis (>60% of hepatocytes) that disappeared completely upon successful antiviral therapy, thus proving its viral origin. All other patients lacked significant fatty liver, despite high levels of HCV replication relative to the patient with genotype 3a (Table 1).

2.2. Plasmid construction

HCV RNA was isolated from snap-frozen liver biopsy specimens (patients #1–5) or serum (patient #6) with Trizol™ reagent (Invitrogen AG, Basle, Switzerland). The complete HCV core-encoding region was reverse transcribed with AMV reverse transcriptase (Promega, Wallisellen, Switzerland), and amplified by PCR using High Fidelity Taq polymerase (Roche, Rotkreuz, Switzerland). Amplicons were cloned using appropriate restriction sites into the bicistronic pIRES2-EGFP vector (Clontech).

Following transformation, plasmids were purified using the Qiafilter Midi purification kit (Qiagen, Basle, Switzerland).

Direct sequencing of the expression vectors was carried out using the ABI Prism 377 DNA sequencer and primers complementary to the 5' and 3' regions of the multiple cloning site. Sequences were aligned using the Multalin program [21].

2.3. Transfections

Human hepatoma cells Huh7 were maintained in Dulbecco's modified Eagle medium (DMEM) supplemented with 10% heat-inactivated fetal bovine serum (FBS), 100 U/ml penicillin G and 100 µg/ml streptomycin sulfate. Plasmids were transfected into Huh7 cells with Lipofectamine 2000 and incubated at 37 °C with Optimem medium for the first 6 h from transfection in a humidified, 5% CO₂ incubator. The medium was then changed to DMEM containing 10% FCS without antibiotics and incubated for another 42 h, when HCV core protein expression and triglyceride level measurements were carried out. All products were from Invitrogen (Basle, Switzerland). In selected experiments, cells were incubated for 48 h before transfection and throughout thereafter in delipidated calf bovine serum (Sigma, Steinheim, Germany).

2.4. Antibodies

Monoclonal antibody C7-50 against the core protein was a kind gift from Dr D. Moradpour (Freiburg, Germany). Mouse monoclonal antibodies against β-actin and the FLAG epitope were kindly provided by Drs C. Chaponnier and B. Conne, respectively (Geneva, Switzerland).

2.5. Indirect immunofluorescence (IFL)

Huh7 cells, grown and transfected on coverslips, were fixed for 30 min in 4% paraformaldehyde at 4 °C. Coverslips were then washed three times in PBS and incubated with the C7-50 antibody diluted 1:300 in PBS, 2% bovine serum albumin (BSA), 1.2% Triton X-100 for 2 h at room temperature (RT). After three washes in PBS, cells were incubated 2 h at RT with Alexa Fluor 530-conjugated goat anti-mouse IgG (Molecular Probes, Juro AG, Lucerne, Switzerland), for light microscopy, or with a rhodamin-conjugated sheep anti-mouse IgG (Chemicon International Inc., Juro AG), for confocal microscopy, both diluted 1:300 in PBS, 0.5% BSA. After rinsing three times in PBS, lipids were stained with Oil Red O (ORO) in 40% isopropanol for 2 min. After further rinsing twice in PBS, coverslips were mounted on microscope slides. For confocal microscopy, slides mounted for immunofluorescence were observed using a Zeiss LSM 510 microscope.

2.6. Lipid enzymatic dosage

Cells were trypsinized 48 h after transfection and counted in a Neubauer chamber. GFP-expressing cells were sorted by flow cytometry using FACS VantageSE (Becton Dickinson, Franklin Lakes, NJ, USA). Twenty-thousand cells were lysed in 35 µl of 0.01% digitonin (kind gift of Dr D. Belin, Geneva) and gently shaken at RT for 45 min. Triglycerides were enzymatically quantified by a commercially available kit (Bioreac, Lausanne, Switzerland). Levels of triglycerides per 20,000 cells were expressed as O.D. readings at 546 nm.

Table 1
Features of the six chronic hepatitis C patients from whom the isolates used in the present study were derived

| # | Type | Age | Gender | Geographic origin | Liver steatosis | Serum HCV RNA (IU/ml) | Liver (–) HCV RNA | Response to therapy |
|---|------|-----|--------|-------------------|-----------------|-----------------------|-------------------|---------------------|
| 1 | 1b | 41 | M | Switzerland | No | 950,000 | 64 | NR |
| 2 | 2a | 44 | M | Ivory Coast | No | 4,900,000 | 2 | Untreated |
| 3 | 3a | 49 | M | Switzerland | Severe | 450,000 | 64 | Responder |
| 4 | 3h | 36 | M | Somalia | No | 643,000 | 2 | Untreated |
| 5 | 4h | 62 | F | Congo | No | 8,000,000 | 64 | NR |
| 6 | 5a | 42 | F | Mozambique | No | 1,720,000 | NA ^a | Untreated |

^a NA, not available.

2.7. Immunoblot detection of HCV proteins

Huh7 cells were lysed in a 2× buffer containing 250 mM Tris–HCl, pH 6.8, 500 mM DTT, 10% SDS, 0.5% bromophenol blue and 50% glycerol. Samples (20,000 cells) were boiled, loaded on 15% polyacrylamide gel and separated by electrophoresis. Protein transfer was performed on nitrocellulose membrane (Milia, Geneva, Switzerland). Membranes were blocked with 5% skim milk in wash buffer, containing 0.05% sodium azide and incubated with the primary antibody C7-50, anti β-actin or anti-FLAG in blocking solution, at appropriate dilutions. Following three washes in wash buffer (20 mM Tris–HCl, pH 7.6, 140 mM NaCl, 0.1% Tween 20), membranes were incubated with a secondary horseradish peroxidase-conjugated antibody (BioRad) diluted 1:3000 in wash buffer. After three further washes, proteins were revealed by chemiluminescence (ECL, Amersham-Pharmacia Biotech, Freiburg, Germany) and the signal detected on an X-ray film. For quantitative measurement, the film was scanned by densitometry, and the spots corresponding to β-actin, HCV core and FLAG-core fusion protein were analysed using the NIH-Image analysis program Scion IMAGE (Scion Corp., Frederick, MD, USA).

2.8. Statistics

Differences were evaluated by the Student's *t* test for parametric variables.

3. Results

3.1. Construction of the HCV core-encoding consensus sequence

Fig. 1 shows the alignment of the six core-encoding consensus sequences considered. The genotypes 3a and 3h

differed from each other by as many as 8.9% of residues, as previously reported [19]. The two prolines at positions 138 and 143, required for association of the core protein with lipids [23], are conserved across all genotypes. The YATG motif (residues 164–7), located in the central domain, shared with the plant protein oleosin and required for lipid association [23], is also conserved, with the exception of a phenylalanine replacing the tyrosine 164 in genotype 3a.

Sequences were inserted in a bicistronic pIRES2-EGFP eukaryotic expression vector. The efficiency of transfection (percentage of GFP-positive cells) was comparable across the different experiments (~30%), with the exception of genotype 1b, which was consistently lower (~15%).

3.2. The core protein induces lipid accumulation

We assessed the core protein expression (by IFL) and lipid staining (by ORO staining) 48 h after transfection (Fig. 2). At this time, lipid droplets were focally amassed in the cytoplasm, mostly in the perinuclear space (Fig. 2B and E). The pattern of lipid staining observed in core-expressing cells was clearly distinct from that displayed at baseline, i.e. in non-transfected Huh7 cells, where minute lipid droplets are typically dispersed throughout the cytoplasm (Fig. 2F).

The percentage of ORO-positive cells among HCV-transfected cells was significantly higher than in untransfected cells for all genotypes ($P < 0.001$ for types 1b, 3a,

| | | | | | | | |
|----|-----------------------------|----------------------|-------------------------------------|---------------------|--------------------------------------|---|----------|
| | 1 | | | | 50 | | |
| 1b | MSTNPKPQRK | TKRNTNRRPQ | DVKFPPGGGQI | VGGVYLLPRR | GPRLGVRAPR | | |
| 2a | MSTNPKPQRK | TKRNTNRRPQ | DVKFPPGGGQI | VGGVYLLPRR | GPRLGVRATR | | |
| 3a | MST L PKPQRK | TKRNT I RRPQ | DVKFPPGGGQI | VGGVY V LPRR | GPRLGV C ATR | | |
| 3h | MST L PKPQRK | TKRNT I RRPQ | N VKFP P GGGQI | VGGVY V LPRR | GP T LGVR A AR | | |
| 4h | MSTNPKPQRK | TKRNTNRR P M | DVKFPPGGGQI | VGGVYLLPRR | GPRLGVRATR | | |
| 5a | MSTNPKPQRK | TKRNT S RRPQ | DVKFPPGGGQI | VGGVYLLPRR | GPR M GVRATR | | |
| | 51 | | | | 100 | | |
| 1b | KTSESRQPRG | RRQPIPKARR | P EGR T WAQPG | YPWPLYGNEG | M GWAGWLLSP | | |
| 2a | KTSESRQPRG | RRQPIPK D PR | S TGR S WGRPG | YPWPLYGNEG | L GWAGWLLSP | | |
| 3a | KTSESRQPRG | RRQPIPKARR | SEGRSWAQPG | YPWPLYGNEG | CGWAGWLLSP | | |
| 3h | KTSESRQPRG | RRQPIPKARR | N EGR T WAQPG | YP S LYGNEG | CGWAGWLLSP | | |
| 4h | KTSESRQPRG | RRQPIPKARP | SEGRSWAQPG | YPWPLYGNEG | CGWAGWLLSP | | |
| 5a | KTSESRQPRG | RRQPIPKAR Q | S TGR S W Q PG | YPWPLY A NEG | L GWAGWLLSP | | |
| | 101 | | | | 150 | | |
| 1b | RGSRPSWGP T | DPRRRSRNLG | KVIDTLTCGF | ADLMGYIPLV | GAP L GG A AARA | | |
| 2a | RGSRPSWGP T | DPR H RRSRNLG | KVIDTLTCGF | ADLMGYI P VV | GAPVGGV A RA | | |
| 3a | RGSRPSWGP N | DPRRRSRNLG | KVIDTLTCGF | ADLMGYIPLV | GAPVGGV A RA | | |
| 3h | RGSRP H WGP N | DPRRRSRNLG | K I I DTLTCGF | ADLMGYIPLV | GAPVGGV A RA | | |
| 4h | RGSRPSWGP N | DPRRRSRNLG | KVIDTLTCGF | ADLMGYIPLV | GAPVGGV A RA | | |
| 5a | RGSRP N WGP N | DPRRRSRNLG | KVIDTLTCGF | ADLMGYIPLV | G GPVGGV A RA | | |
| | 151 | | | | 191 | | |
| 1b | LAHGVR V LED | G V N | YATG | NLP | GCSFSIFLLA | LLSCL T IPAS | A |
| 2a | LAHGVR V LED | GIN | YATG | NLP | GCSFSIFLLA | LLSCL I SVPV S | A |
| 3a | LAHGVR A LED | GIN | F ATG | NLP | GCSFSIFLLA | L F S CL V HP A A | S |
| 3h | LAHGVR A VED | GIN | YATG | NLP | GCSFSIFLLA | LLSCL T VPAS | G |
| 4h | LAHGVR A LED | GIN | YATG | NLP | G A F S I F LLA | LLSCL T VPAS | A |
| 5a | LAHGVR A LED | G V N | YATG | NLP | GCSFSIF I L A | LLSCL T VPAS | A |

Fig. 1. Alignment of the consensus sequences of the core-encoding region belonging to the six HCV subtypes used in the present study. The HCV core domain 2 is underlined. The two prolines 138 and 143 are in bold. The YATG motif is boxed.

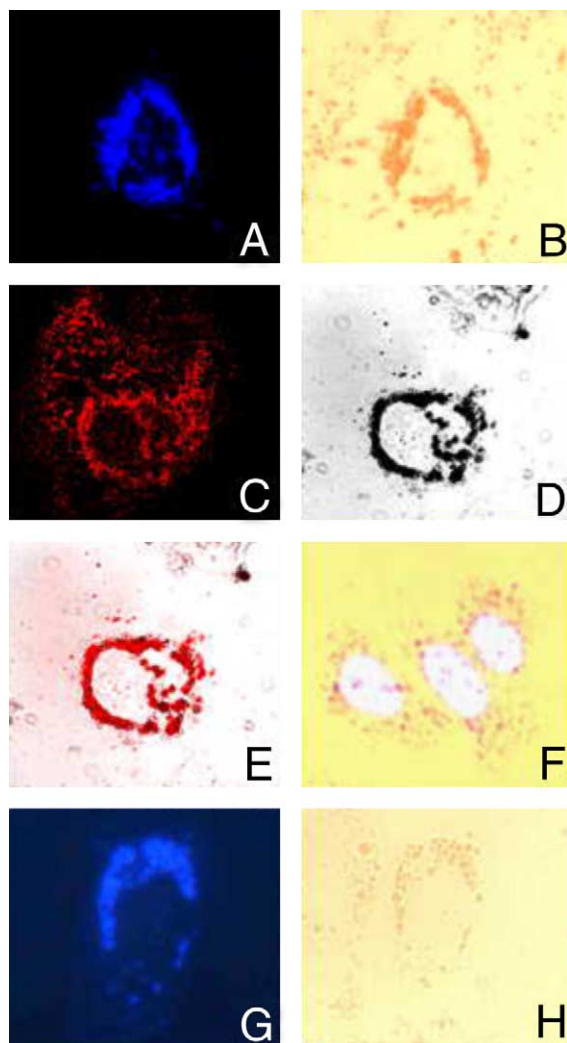


Fig. 2. Microphotographs of Huh7 cells before (F) and 48 h after transfection with the HCV core protein of genotype 3a (A–E, G,H), both by light microscopy (A,B; F–H) and by confocal microscopy (C–E). The HCV core expression is detected by IFL (A,C,E,G) and the lipid accumulation pattern by Oil Red O staining (B,D,E,H). Photographs in G and H show HCV core expression and lipid accumulation in Huh7 cells transfected in delipidated medium. For further explanations, please refer to text.

3h, 5a; $P=0.002$ for type 2a; $P=0.021$ for type 4h) (Fig. 3). However, the lipid droplets were found more often in cells expressing the core protein 3a ($77.6 \pm 6.3\%$ of transfected cells) and 3h ($82.3 \pm 11.6\%$) as compared to 1b ($34.3 \pm 4.7\%$) and to all remaining genotypes ($P < 0.001$) (Fig. 3). The proportion of lipid amassing cells among control GFP-transfected cells was not significantly different from GFP-negative cells. Similarly, the proportion of core-transfected cells showing lipid droplets was significantly higher than seen in control cells transfected with the GFP protein alone, except in case of transfection with genotype 4h (6.6 ± 4.4 ; $P < 0.001$ vs. types 3a and 3h; $P=0.002$ vs. type 1b; $P=0.009$ vs. type 5a; $P=0.038$ vs. type 2a) (Fig. 3).

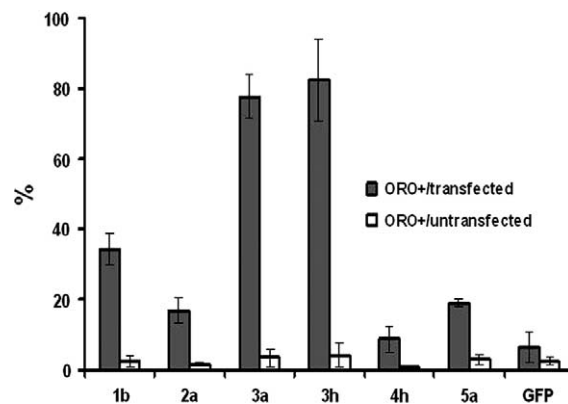


Fig. 3. Percentage of Oil Red O (ORO)-stained cells over HCV core (or GFP) positive (grey boxes) vs. negative (white boxes) Huh7 cells, after transfection with the HCV core of genotypes 1b, 2a, 3a, 3h, 4h and 5a or with GFP. Data are means \pm SD of at least three independent experiments.

3.3. Quantification of triglycerides in transfected cells

To distinguish intracellular redistribution of fat from true lipid accumulation, we measured the total amount of triglycerides in transfected vs. untransfected cells. GFP-positive cells were separated by flow cytometry, and lipids were extracted from 20,000 transfected or, respectively, untransfected cells. Optical densities obtained after enzymatic measurement of triglycerides at 546 nm are graphically represented in Fig. 4A. The level of triglycerides was significantly higher in transfected vs. untransfected cells only for genotypes 1b ($P=0.015$), 3a ($P=0.003$) and 3h ($P=0.025$), but not for the remaining genotypes. The level of triglycerides was significantly higher in cells transfected with the genotype 3a (Fig. 4A) as compared to genotypes 1b and 3h, whereas in cells transfected with genotypes 2a, 4h and 5a it was comparable to the level measured in untransfected cells.

To better quantify the relative accumulation of triglycerides in genotype 3a, we performed a reference standard curve. Serially diluted amounts of cells transfected with genotype 3a and sorted by FACS were mixed with increasing amounts of untransfected Huh7 cells, to reach a total of 20,000 cells in each quantified sample, and triglycerides were then measured on all mixtures. According to Fig. 4B, triglycerides were quantified over a linear range encompassing 7500–20,000 transfected cells. Extrapolation of these results to those shown in Fig. 3 allowed us to conclude that transfection with genotype 3a resulted in a triglyceride accumulation about three-fold with respect to genotype 1b and about two-fold as compared with genotype 3h.

3.4. Detection of the HCV core protein by immunoblot

To exclude that the different level of lipid accumulation was due to a different level of core protein expression, we

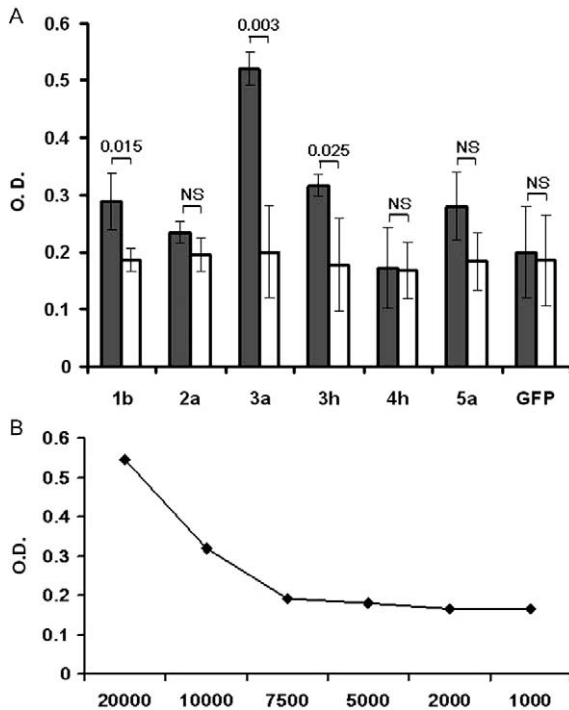


Fig. 4. (A) Triglyceride measurements in 20,000 core- or GFP-expressing Huh7 cells (grey boxes) or untransfected cells from the same experiments (white boxes), expressed as O.D. measured at 546 nm, after transfection with the HCV core of genotypes 1b, 2a, 3a, 3h, 4h and 5a or the GFP. (B) Reference curve of triglycerides dosage: 20,000, 10,000, 7500, 5000, 2000 or 1000 Huh7 cells transfected with HCV core 3a were mixed with increasing amounts of untransfected Huh7 cells to a final of 20,000 cells and subjected to enzymatic measurement of triglyceride content (see text). Data are means \pm SD of at least three independent experiments.

quantified the latter by immunoblot on equal amounts of FACS-sorted cells (Fig. 5A). Following normalization to β -actin, and assuming the amount of genotype 3a core protein equal to 1, data show that the expression of the remaining genotypes was generally higher, with the exception of type 3h (Fig. 5A). However, to rule out a measurement bias due to a variable affinity of the antibody towards the HCV core proteins of different genotypes, we also expressed the FLAG-core fusion proteins corresponding to genotypes 1b, 3a and 3h (i.e. the three genotypes associated with a true accumulation of triglycerides). The expression level of these fusion proteins, as assessed by an anti-FLAG antibody, was comparable (Fig. 5B). These results were confirmed by stripping and re-blotting with the C7-50 anti-HCV core the same membrane used for quantification of the FLAG-core fusion proteins (data not shown).

3.5. Lipid accumulation in delipidated medium

We assessed whether triglyceride accumulation may occur also in the presence of delipidated culture medium.

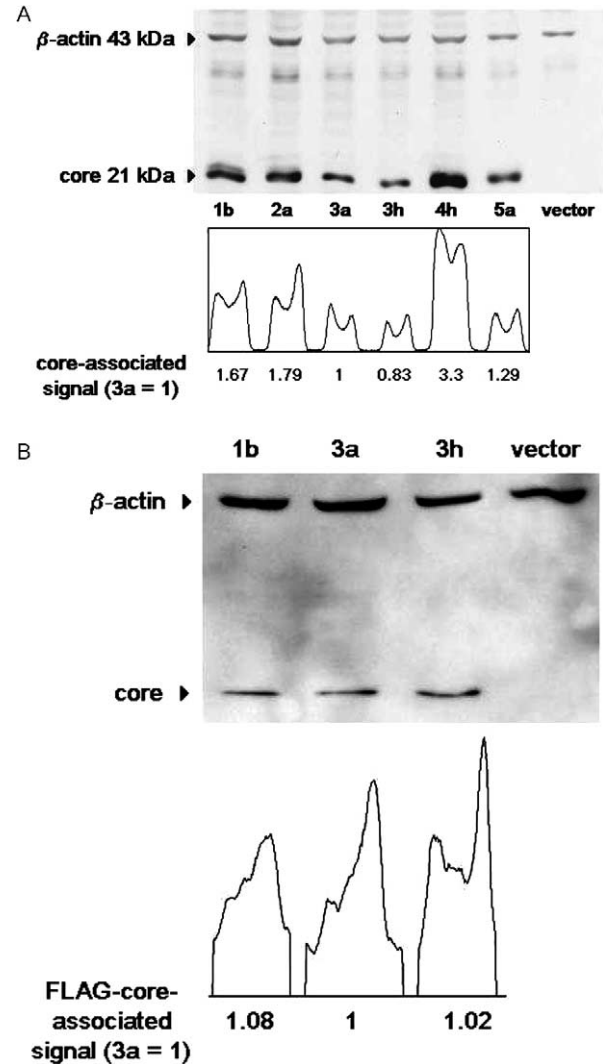


Fig. 5. (A) Immunoblot detection of the HCV core protein of genotypes 1b, 2a, 3a, 3h, 4h and 5a (top panel). Measurement of the HCV core-associated signal by densitometry (bottom panel). Levels are relative to HCV genotype 3a (taken as a reference = 1). (B) Immunoblot detection of the FLAG-core fusion proteins derived from genotypes 1b, 3a and 3h (top panel). Measurement of the fusion protein-associated signal by densitometry (bottom panel). Levels are relative to the FLAG-core fusion protein derived from genotype 3a (taken as a reference = 1).

After conditioning cells for 48 h with lipid-free medium, we carried out the transfection with the core protein of genotype 3a, and measured the level of intracellular triglycerides in 20,000 transfected vs. 20,000 untransfected cells, as separated by flow cytometry. As shown in Fig. 2H and 6, cells failed to significantly accumulate triglycerides under these conditions. The immunoblot quantification of the core protein showed also a reduction of viral protein expression of 0.61-fold, as compared to the level found in cells grown in lipid-containing medium, possibly due to a decreased cellular metabolism following cultivation in a lipid-depleted medium.

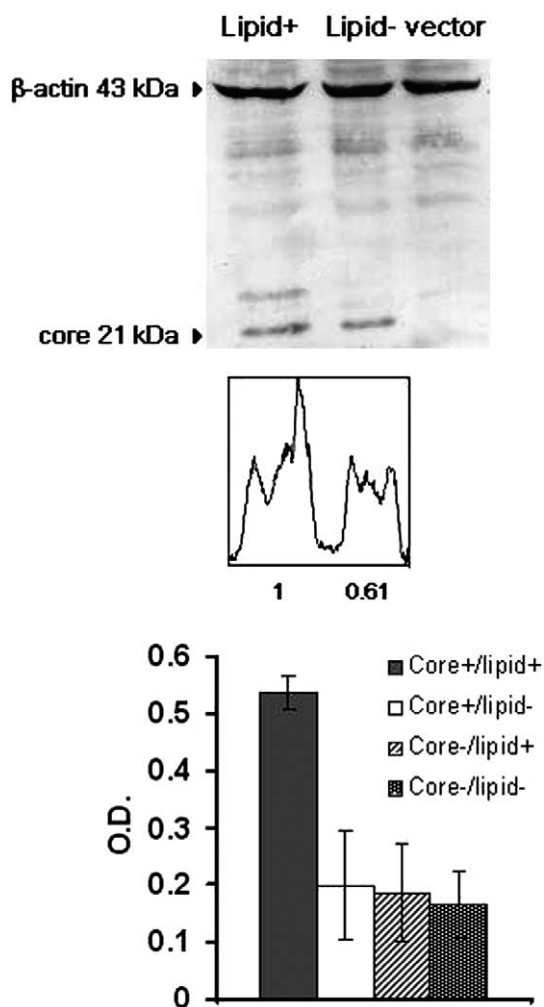


Fig. 6. Immunoblot detection of the HCV core protein of genotype 3a in delipidated medium (lane 'lipid-'), as compared to the core detected upon transfection of the control cell line (lane 'lipid+') (top panel). Measurement of the HCV core-associated signal by densitometry (center panel). Triglycerides measurement in Huh7 cells transfected with the HCV core protein 3a (grey and white boxes) or untransfected (dashed and black boxes), with ('lipid+') or, respectively, without lipids ('lipid-') in the culture medium (bottom panel).

4. Discussion

Previous data have suggested that the HCV core protein is associated with lipid droplets *in vitro* [15–17] and is sufficient to induce liver steatosis in transgenic mice [14]. These observations were made using viral sequences of genotype 1, without providing information on the liver histology of patients from which such isolates were derived. In chronic hepatitis C, steatosis is significantly associated with genotype 3a, although also patients with other genotypes may have virally-induced fatty liver. To ascertain which viral construct may provide the ideal model to study HCV-associated steatosis, we expressed *in vitro* the HCV core-encoding sequences isolated from chronic hepatitis C patients with different genotypes and well-characterized liver histology. All these constructs (but not the control

vector) promoted the appearance of lipid droplets in the perinuclear space of transfected cells, some genotypes (1b, 3a and 3h) being more efficient than others (2a, 4h and 5a). Droplets colocalized with the HCV core protein, as detected by immunofluorescence, in agreement with previous data [17–19]. However, when we measured the level of triglycerides in the same cells, transfection induced a significant accumulation only with the viral constructs of genotypes 1b, 3a and 3h. This suggests that in the case of transfection with genotypes 2a, 4h and 5a, the core protein seems to promote a mere redistribution of fat-laden vesicles typically found in Huh7 cells (Fig. 2F), rather than a true triglyceride accumulation. In addition, the measurement of the level of expression of the core protein allowed us to confirm that genotype 3a is the most efficient in terms of triglycerides accumulation, leading to levels that are three-fold as compared to those caused by genotype 1b, and about two-fold as compared to those of genotype 3h.

These results only partially confirm the features reported in the chronic hepatitis C patients from which we derived the isolates used for transfection. In fact, although our genotype 3a-derived construct was the most efficient to induce triglyceride accumulation, also the construct derived from patient #1 (i.e. infected by HCV genotype 1b) caused some degree of accumulation, despite the absence of steatosis in his liver and the high viral load in his serum (Table 1). For what reason this isolate caused triglyceride accumulation in Huh7 cells and not in the liver from which it was derived is unknown. We speculate that other viral proteins (e.g. NS5A) may modulate the steatosis phenotype *in vivo* [19], or that the core protein expressed *in vitro* may not be identical to that predominant in the original liver, due to lack of post-translational modifications in the Huh7 clone used for transfection experiments or to cloning artifacts. This same issue holds true also for the isolate of genotype 3h (patient #4, Table 1). In the case of the remaining genotypes, the phenotype observed in transfected cells mirrored that of the corresponding patients.

Thus, our simple and reproducible transfection system may pave the way for a detailed analysis of the mechanisms underlying the HCV-associated triglyceride accumulation and of the viral sequences responsible for such accumulation. In addition, co-transfection experiments will also assess if any other viral protein may modulate the steatogenic efficiency of genotypes 1b, 3a and 3h. Finally, experiments using untransfected vs. cells transfected with the various HCV genotypes may allow to describe the transcription profiles associated with different phenotypes (triglyceride accumulation or lack thereof) and viral genotypes.

The simple comparison of the consensus sequences of genotypes 1b, 3a and 5a did not allow to identify single aminoacid changes that may account for their differential steatogenic efficiency at equal level of HCV replication. In particular, there were no significant changes within the central domain, whose role in lipid association has been

shown previously [22]. The central domain of the HCV core protein encompasses the region from residue 121 until the C-terminus extremity of the mature core protein (i.e. around aminoacid 174). Mutagenesis experiments have shown that this central domain is responsible for the lipid association, possibly via hydrophobic interaction with lipid vesicles [22]. Sequence similarities were found between this domain and that involved in lipid association of oleosin, a plant protein capable of binding to lipid droplets [23]. Site-directed mutagenesis experiments in the central domain of the HCV core protein have shown that the two prolines at positions 138 and 143 and a YATG motif, also located in domain 2 and shared with oleosin, are required for lipid association [23]. Both proline residues were conserved throughout all genotypes used in the present study. The YATG motif was conserved in all our constructs except for genotype 3a, where a tyrosine was substituted for by a phenylalanine, but our preliminary site-directed mutagenesis experiments have so far failed to associate this particular sequence with the steatogenic phenotype (data not shown). Thus, the identification of steatogenic sequences may require a complex combination of cassettes among steatogenic and non-steatogenic genotypes.

Growing cells in delipidated medium suppressed the triglycerides accumulation induced by genotype 3a, suggesting the lack of ex novo synthesis of triglycerides induced by the viral protein, and confirming that a blockade exists in the recycling of fatty acids imported by hepatocytes and re-exported under forms of secreted lipoproteins. This observation is compatible with previous data showing that HCV core protein blocks the VLDL assembly both in humans [24,25] and in transgenic mice [26], and further strengthens the significance of the present model to study human pathology.

In conclusion, the pattern observed in Huh7 cells upon expression of the six core proteins largely corroborated the phenotype seen in vivo. The genotype 3a-derived core protein is about three-fold more efficient than the corresponding protein from genotype 1b to induce triglycerides accumulation in transfected cells, and is therefore the ideal candidate to study the pathogenesis of HCV-induced steatosis.

Acknowledgements

This study was supported by Grants 3200-63549.00 and 3200B0-103727 from the Swiss National Science Foundation.

References

- [1] National Institutes of Health Consensus Development Conference. Management of hepatitis C. *Hepatology* 2002;36:S1–S252.
- [2] Poynard T, Mathurin P, Lai CL, Guyader D, Poupon R, Tainturier MH, et al. A comparison of fibrosis progression in chronic liver diseases. *J Hepatol* 2003;38:257–265.
- [3] Hourigan LF, MacDonald GA, Purdie D, Whitehall VH, Shorthouse C, Clouston A, et al. Fibrosis in chronic hepatitis C correlates significantly with body mass index and steatosis. *Hepatology* 1999;29:1215–1219.
- [4] Zarski JP, Bohn B, Bastie A, Pawlowsky JM, Baud M, Bost-Bezeaux F, et al. Characteristics of patients with dual infection by hepatitis B and C viruses. *J Hepatol* 1998;28:27–33.
- [5] Benhamou Y, Bochet M, Di Martino V, Charlotte F, Azria F, Coutellier A, et al. Liver fibrosis progression in human immunodeficiency virus and hepatitis C virus coinfecting patients. The Multivirc Group. *Hepatology* 1999;30:1054–1058.
- [6] Adinolfi LE, Gambardella M, Andreana A, Tripodi MF, Utili R, Ruggiero G. Steatosis accelerates the progression of liver damage of chronic hepatitis C patients and correlates with specific HCV genotype and visceral obesity. *Hepatology* 2001;33:1358–1364.
- [7] Westin J, Nordlinder H, Lagging M, Norkrans G, Wejstal R. Steatosis accelerates fibrosis development over time in hepatitis C virus genotype 3 infected patients. *J Hepatol* 2002;37:837–842.
- [8] Monto A, Alonzo J, Watson JJ, Grunfeld C, Wright TL. Steatosis in chronic hepatitis C: relative contributions of obesity, diabetes mellitus, and alcohol. *Hepatology* 2002;36:729–736.
- [9] Rubbia-Brandt L, Fabris P, Paganin S, Leandro G, Male P-J, Giostra E, et al. Steatosis affects chronic hepatitis C progression in a genotype specific way. *Gut* 2004;53:406–412.
- [10] Poynard T, Ratzu V, McHutchison J, Manns M, Goodman Z, Zeuzem S, et al. Effect of treatment with peginterferon or interferon alfa-2b and ribavirin on steatosis in patients infected with hepatitis C. *Hepatology* 2003;38:75–85.
- [11] Hui JM, Sud A, Farrell GC, Bandara P, Byth K, Kench JG, et al. Insulin resistance is associated with chronic hepatitis C and virus infection fibrosis progression. *Gastroenterology* 2003;125:1695–1705.
- [12] Goodman ZD, Ishak KG. Histopathology of hepatitis C virus infection. *Semin Liver Dis* 1995;15:70–81.
- [13] Rubbia-Brandt L, Quadri R, Abid K, Giostra E, Male PJ, Mentha G, et al. Hepatocyte steatosis is a cytopathic effect of hepatitis C virus genotype 3. *J Hepatol* 2000;33:106–115.
- [14] Kumar D, Farrell GC, Fung C, George J. Hepatitis C virus genotype 3 is cytopathic to hepatocytes. Reversal of hepatic steatosis after sustained therapeutic response. *Hepatology* 2002;36:1266–1272.
- [15] Rubbia-Brandt L, Giostra E, Mentha G, Quadri R, Negro F. Expression of liver steatosis in hepatitis C virus infection and pattern of response to alpha-interferon. *J Hepatol* 2001;35:307.
- [16] Moriya K, Yotsuyanagi H, Shintani Y, Fujie H, Ishibashi K, Matsuura Y, et al. Hepatitis C virus core protein induces hepatic steatosis in transgenic mice. *J Gen Virol* 1997;78:1527–1531.
- [17] Barba G, Harper F, Harada T, Kohara M, Goulinet S, Matsuura Y, et al. Hepatitis C virus core protein shows a cytoplasmic localization and associates to cellular lipid storage droplets. *Proc Natl Acad Sci USA* 1997;94:1200–1205.
- [18] Hope RG, McLauchlan J. Sequence motifs required for lipid droplet association and protein stability are unique to the hepatitis C virus core protein. *J Gen Virol* 2000;81:1913–1919.
- [19] Shi ST, Polyak SJ, Tu H, Taylor DR, Gretch DR, Lai MM. Hepatitis C virus NS5A colocalizes with the core protein on lipid droplets and interacts with apolipoproteins. *Virology* 2002;292:198–210.
- [20] Abid K, Quadri R, Veuthey AL, Hadengue A, Negro F. A novel hepatitis C virus (HCV) subtype from Somalia and its classification in HCV clade 3. *J Gen Virol* 2000;81:1485–1493.
- [21] Corpet F. Multiple sequence alignment with hierarchical clustering. *Nucleic Acids Res* 1988;16:10881–10890.

- [22] Hope RG, McLauchlan J. Sequence motifs required for lipid droplet association and protein stability are unique to the hepatitis C virus core protein. *J Gen Virol* 2000;81:1913–1925.
- [23] Hope RG, Murphy DJ, McLauchlan J. The domains required to direct core proteins of hepatitis C virus and GB virus-B to lipid droplets share common features with plant oleosin proteins. *J Biol Chem* 2002;277:4261–4270.
- [24] Serfaty L, Andreani T, Giral P, Carbonell N, Chazouillères O, Poupon R. Hepatitis C virus induced hypobetalipoproteinemia: a possible mechanism for steatosis in chronic hepatitis C. *J Hepatol* 2001;34:428–434.
- [25] Hofer H, Bankl HC, Wrba F, Steindl-Munda P, Peck-Radosavljevic M, Osterreicher C, et al. Hepatocellular fat accumulation and low serum cholesterol in patients infected with HCV-3a. *Am J Gastroenterol* 2002;97:2880–2885.
- [26] Perlemuter G, Sabile A, Letteron P, Vona G, Topilco A, Chretien Y, et al. Hepatitis C virus core protein inhibits microsomal triglyceride transfer protein activity and very low density lipoprotein secretion: a model of viral-related steatosis. *Fed Am Soc Exp Biol J* 2002;16: 185–194.